

Vortex Shedding From Circular and Rectangular Cylinders Placed Horizontally in a Turbulent Flow

Mustafa SARIOGLU & Tahir YAVUZ

*Department of Mechanical Engineering,
Karadeniz Technical University,
61080 Trabzon-TURKEY
e-mail : sarioglu@ktu.edu.tr*

Received 07.03.1999

Abstract

In this study, vortex sheddings from cylinders of circular and rectangular cross-sections of finite length which spanned the mid-height of the test section of a horizontal wind tunnel, were determined experimentally. Three rectangular models having width-to-height ratios of 0.5, 1.0 and 2.0 were considered. Hot-film measurements in the wake of these models were carried out at Reynolds numbers in the range $1 \times 10^4 - 2 \times 10^5$. From these measurements, spectral density distributions depending on models width-to-height ratio, blockage, angle of incidence and Reynolds number in the wake were determined.

Key Words: Vortex- Shedding, Bluff Body, Wake Flow, Bluff Body Aerodynamic.

Türbülanslı Akış Yatay Yerleştirilmiş Dairesel ve Dikdörtgen Silindirler Etrafında Girdap Kopması

Özet

Bu çalışmada, yatay bir rüzgar tünelinin deney kesitinin ortasına akım doğrultusuna dik ve yatay olarak yerleştirilmiş sonlu uzunluktaki dairesel ve dikdörtgen kesitli silindirlere vorteks kopmaları deneysel olarak incelenmiştir. Genişlik/yükseklik oranı 0.5, 1.0 ve 2.0 olan üç dikdörtgen model incelenmiştir. Reynolds sayısının $1 \times 10^4 - 2 \times 10^5$ aralığında modellerin iz bölgesinde kızgın-film ölçümleri gerçekleştirilmiştir. Bu ölçümlerden, modellerin genişlik/yükseklik oranına, blokaja, hücum açısına ve Reynolds sayısına bağlı olarak iz bölgelerindeki spektral yoğunluk dağılımları belirlenmiştir.

Anahtar Sözcükler: Girdap Kopması, Küt Cisim, İz, Akışı, Küt Cisim Aerodinamiği

Introduction

Vortex shedding from bluff cylinders has received an increasing amount of attention since it is associated with many cases of flow-induced structural and acoustic vibrations. Vortex shedding from bluff cylinders, including circular and rectangular-section cylinders, has been investigated in many pa-

pers. These include Gaster (1971), Bearman and Trueman (1972), West and Apelt (1982), Sakamoto and Arie (1983), Farell and Blessmann (1983), and Mukhopadhyay et al. (1992).

In Gasters (1971) paper, experiments on slightly tapered models of circular cross-section have shown that the vortex wake structure exists in a number of

discrete cells having different shedding frequencies. He suggested that at very low Reynolds numbers the vortex structure can tolerate more detuning so that the number of cells is at a minimum. Thus, at sufficiently low speeds it seems probable that the wake exists only as a single cell. It may be for this reason that discontinuities in shedding laws are observed at Reynolds numbers in the range 80-90. In their paper, Bearman and Trueman (1972) presented the measurements of the base pressure coefficient, drag coefficient and Strouhal number of rectangular cylinders. Their results confirm the findings of Nakaguchi et al. (1968), that the drag coefficient rises to nearly 3 when the depth of the section is just over half the width. The flow around the sections was found to be strongly influenced by the presence of trailing-edge corners. It was reported in the paper of West and Apelt (1982) that, for blockage ratios less than 6%, the effects of blockage on pressure distribution and drag coefficient are small and the Strouhal number is unaffected by blockage. For blockage ratios in the range of 6-16%, there is considerable distortion of the flow due to blockage and the effects are complex. In Sakamoto and Aries (1983) paper, measurements of the vortex-shedding behind a vertical rectangular prism and a vertical circular cylinder attached to a plane wall were correlated with the characteristics of a smooth-wall turbulent boundary layer in which they were immersed. In their study, as the aspect ratio was reduced, the type of vortex shedding behind each of the two bodies was found to change from the

Karman-type vortex to the arch-type vortex at an aspect ratio of 2.0 for a rectangular prism and 2.5 for a circular cylinder.

The aim of the present study was to investigate the spectral density distributions and vortex sheddings from circular and rectangular cylinders. The dependence of the vortex shedding phenomenon on the width-to-height ratio of the model, angle of incidence and Reynolds numbers of the flow were determined. The Reynolds number based on the height (or diameter for the circular cylinder) of the model ranged between 1×10^4 and 2×10^5 . The results were compared with the data available in the literature.

Experimental Apparatus and Procedure

The experiments consisted of measurements of vortex shedding frequencies using a hot-film anemometer. The measurement of wake velocities was performed in an open return wind tunnel at the Department of Mechanical Engineering of Karadeniz Technical University. The rectangular working section of the tunnel is 457 mm high, 289 mm wide and 1830 mm long. The tunnel configuration is shown in Figure 1. A circular diffuser is connected to the working section through a transition section in which the rectangular shape of the test section changes to the circular shape of the diffuser. The turbulence intensity of the free stream was measured at less than 0.4%, and the uniformity of velocity in the test section was found to be 0.2%.

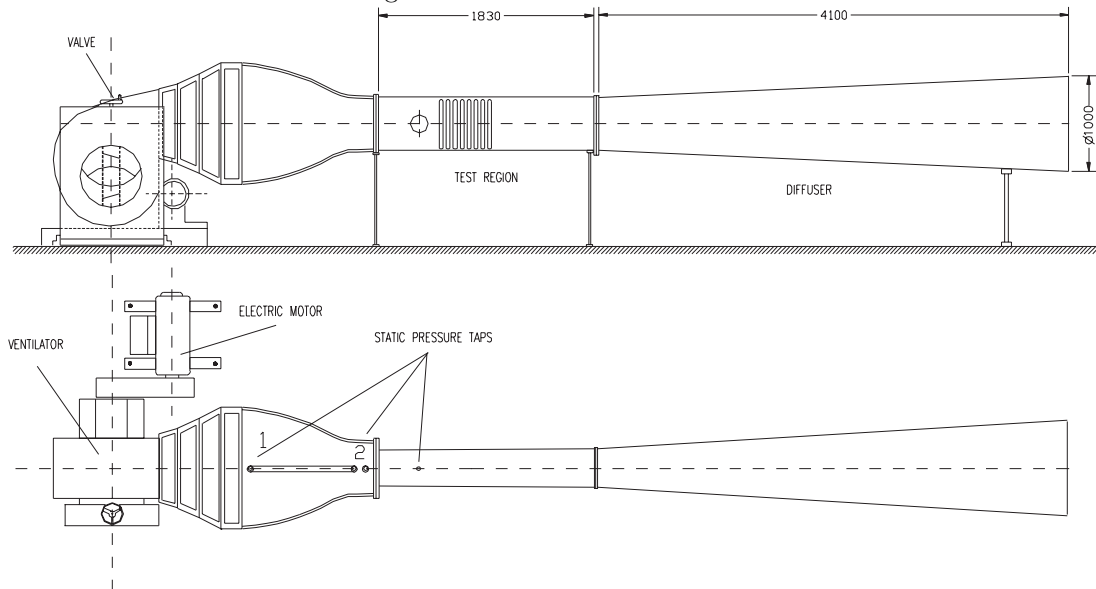


Figure 1. Low-turbulence wind tunnel and test section; all dimensions are in millimeters.

Three rectangular wooden cylinders with width-to-height ratios, w/h , of 0.5, 1.0 and 2.0, and a circular wooden cylinder of 50 mm in diameter were used, where w is the length of the side and h is the height of the rectangular cylinder. The models were placed horizontally at mid-height in the working section (see Figure 2), which is 400 mm downstream of the end of the contraction. The blockage ratios were

17.51%, 10.94% and 8.75% at 0° incidence respectively for the rectangular cylinders and 10.94% for the circular cylinder. The lengths of the cylinders were taken to be equal to the width of the wind tunnel test section. Each model was supported outside the test section so as to eliminate the transmission of tunnel vibrations.

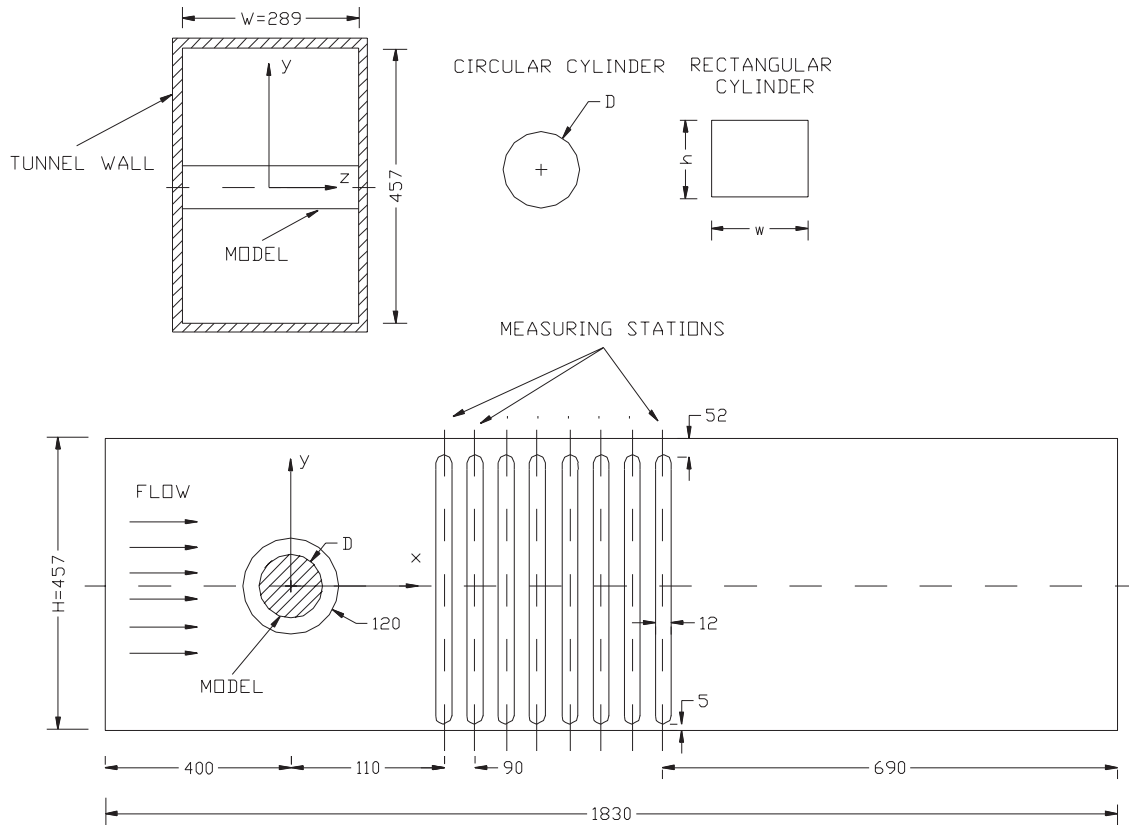


Figure 2. Coordinate system and location of the models; all dimensions are in millimeters.

In the experiments, the velocity fluctuations were detected using a TSI hot-film anemometer. The flow velocity was varied between 5 m/s and 36 m/s, so that the Reynolds number, based on the height (or diameter for the circular cylinder), ranged from 1×10^4 to 2×10^5 .

The vortex-shedding frequency was determined and the Strouhal number $St = f_s h / \bar{U}$ was obtained, where f_s is the dominant vortex shedding frequency, h is the height of the rectangular cylinder and \bar{U} is the mean velocity. A hot-film probe was placed at various positions in the wake of the cylinders. The experimental margin of error in the measurement of velocity was determined to be about ± 0.3 m/s and

that of the positional accuracy of the hot-film probe in the wake was ± 1 mm.

Experimental Results and Discussion

Spectral measurements around circular cylinder

The power spectrum or, more formally, the spectral density function, is a way of representing the frequency content of a signal. The power spectrum tells us what fraction of the signal fluctuations occur in a given frequency band. For a random signal, the power spectrum would tell us the range of frequen-

cies over which oscillations occur and the frequency with the maximum power density. Mathematically, the power spectral density function is defined as:

$$G_x(f) = \lim_{\Delta f \rightarrow 0} \frac{1}{\Delta f} \left\{ \lim_{T \rightarrow \infty} \frac{1}{T} \int_0^T x^2(t, f, \Delta f) dt \right\} \quad (1)$$

In this equation, we see that the expression inside the brackets is the mean square value of the signal $x(t, f, \Delta f)$. The function $x(t, f, \Delta f)$ is just the original signal $x(t)$ filtered around the frequency f with a bandwidth of Δf . The integral is then normalized by this bandwidth.

The spectral densities of axial velocity fluctuations in the wake of the 50 mm diameter circular cylinder were measured at four locations, i) $x/D = 2.2, y/D = 0.5$, ii) $x/D = 2.2, y/D = 1.5$, iii)

$x/D = 4.0, y/D = 0.5$, iv) $x/D = 4.0, y/D = 1.5$, and are given in Figure 3. In the spectra, vortex shedding is reflected by spectral peaks. As shown in this figure, with the increasing Reynolds number, the vortex-shedding frequency increases. It is known that turbulence intensity decreases with the increasing Reynolds number. In these experiments, the turbulence intensities varied from 0.15% to 0.4% in the Reynolds number range considered. Sax (1978) suggested that increasing the intensity of turbulence lowers the frequency of vortex shedding and causes the vortex shedding regimes to occur at lower Reynolds number. In Figures 3a and c, it may be seen that dominant peaks occur about the value of $y/D=0.5$ at the stations $x/D = 2.2$ and 4.0 . Peaks disappear in the spectra when the y/D location for the measurement exceeds 1.5, which is clearly outside the wake of the cylinder.

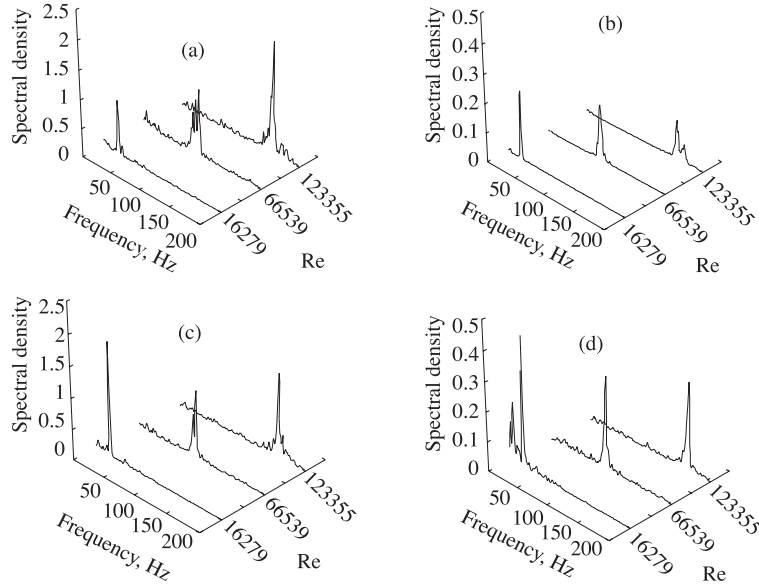


Figure 3. Spectral densities of velocities versus Reynolds number at the positions: a) $x/D = 2.2, y/D = 0.5$ b) $x/D = 2.2, y/D = 1.5$ c) $x/D = 4.0, y/D = 0.5$ d) $x/D = 4.0, y/D = 1.5$ in the wake of circular cylinder.

The Strouhal numbers, $St = f_s D / \bar{U}$ corresponding to the vortex shedding frequencies, f_s , where D is the diameter for the circular cylinder and \bar{U} is the mean free stream velocity, are plotted in Figure 4, together with the data some of other investigators. It may be observed from this figure that the Strouhal numbers reported by various investigators exhibit some scatter, which can be explained in terms of the differences in blockage ratios. The blockage ratios reported in the experiments of Achenbach and

Heinecke (1981), Farell and Blessmann (1983), Kim (1986) and Bearman (1969) were 16.67%, 11.9%, 11.8% and 6.5% respectively, while it was 10.94% in the present work. It was found (Figure 4) that the St number decreased slightly with increasing Reynolds number.

Sometimes, in the literature, a parameter which is called the shedding frequency parameter (non-dimensional frequency), $F = f_s D^2 / \nu$, is calculated using the shedding frequencies, f_s , from spectral den-

sity functions, where ν is the kinematic viscosity of the fluid. The shedding frequency parameter represents the product of the Reynolds number and Strouhal number. Figure 5 shows the variation of the shedding frequency parameter versus Reynolds number at the position $x/D = 4, y/D = 1.5$ together with data found in the literature. As shown in this figure, the shedding frequency parameter increases linearly with the Reynolds number. This increase agrees with the results determined by other investigators (Nishioka and Sato (1974) and Gerich and Eckelmann (1982)). A linear relationship between the vortex shedding frequency parameter and the Reynolds number is obtained in the following form:

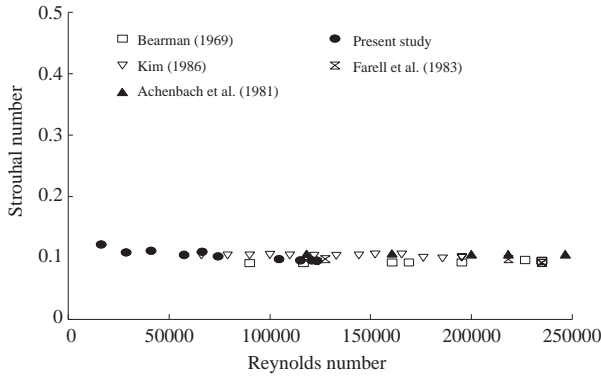


Figure 4. Strouhal numbers versus Reynolds numbers.

$$F = f_s D^2 / \nu = 0.194 \cdot Re + 1006; \quad (2)$$

for $16000 < Re < 124000$

Spectral measurements around rectangular cylinders

Measurements were carried out in the positive and negative sides of the wake of the cylinder at

incidence angles of $0^\circ, 5^\circ, 10^\circ, 20^\circ$ and 30° . The positive and negative sides of the wake are defined as the positive and negative directions of the y-axis respectively, as shown in Figure 2.

The spectral density distributions of velocities in the positive and negative sides of the wake of the square cylinder are calculated from the hot-film signals. The Reynolds number varied from 1.6×10^4 to 1.23×10^5 . The results are shown in Figures 6, 7, 8, 9, and 10.

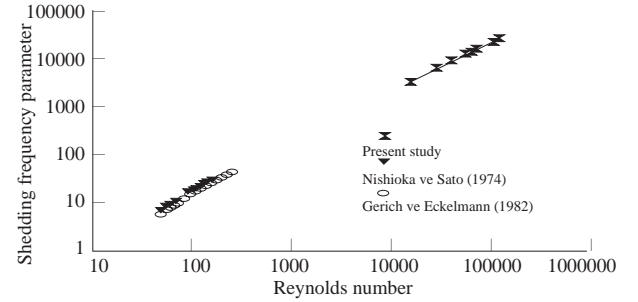


Figure 5. Shedding frequency parameter versus Reynolds number.

The spectral density distributions of velocities versus y/h are shown in Figure 6 for three different Reynolds numbers: 16279, 66539 and 123355. The intensities of the spectral peaks first increase with increasing y/h and reach their maximum values at $y/h=1.0$ and then decrease with increasing y/h . As is shown, the intensity of the spectral peaks diminishes considerably in the region beyond $y/h > 2.5$. In the wake of the circular cylinder having the same hydraulic diameter and the same blockage ratio, the intensity of the spectral peaks diminishes after approximately $y/D > 1.5$. This is because the wake of the circular cylinder is narrower than that of the square cylinder due to the difference in their shapes and the locations of the flow separation points.

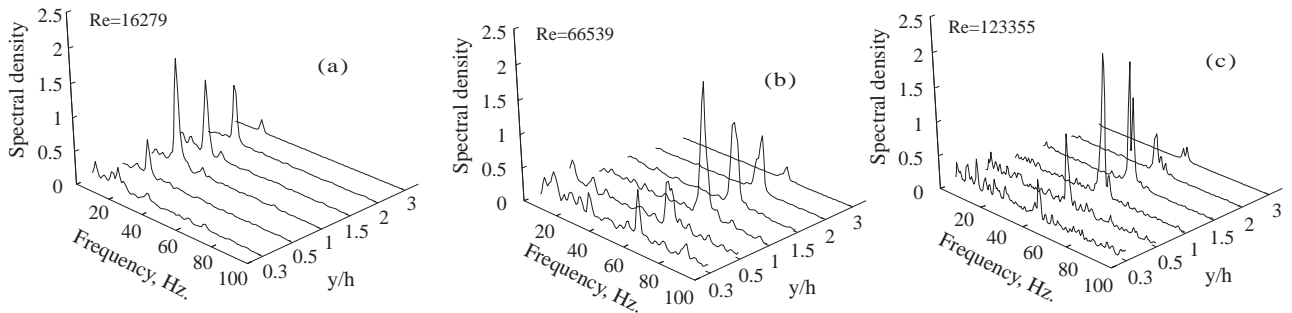


Figure 6. Spectral densities of velocities versus y/h at station $x/h=4.0$ for square cylinder at 0° incidence.

Spectral density distributions of velocities obtained in the positive and negative sides of the wake of the square cylinder at different angles of incidences; 0, 5, 10, 20 and 30 degrees, are presented in Figures 7, 8, 9, and 10. As it may be seen from these figures, for the three Reynolds numbers considered, the angle of incidence has very little effect on the vortex shedding frequencies for the square cylinder. Comparing Figures 7 and 8, which represent the results obtained at $x/h = 4.0, y/h = 0.5$ and $x/h = 4.0, y/h = -0.5$, it can be observed that the intensity of the spectral peaks increases with the increasing angle of incidence and reaches the maximum values at $\alpha = 30^\circ$ for Reynolds numbers 16279 and 66539. In addition, one dominant and

single spectral peak was detected at this angle in both cases. In the case of a higher Reynolds number of 1.23×10^5 , the intensity of the spectral peaks first decreases and then increases with the increasing angle of incidence. It may also be observed that the intensities of the spectral peaks in Figure 8 detected in the negative side of the wake of the cylinder, $x/h = 4.0, y/h = -0.5$, are higher than the intensities of those detected in the positive side of the wake, $x/h = 4.0, y/h = 0.5$, as shown in Figure 7.

The same trends can be observed in Figures 9 and 10, which represent the measurements performed at the locations $x/h = 4.0, y/h = 1.5$ and $x/h = 4.0, y/h = -1.5$ respectively.

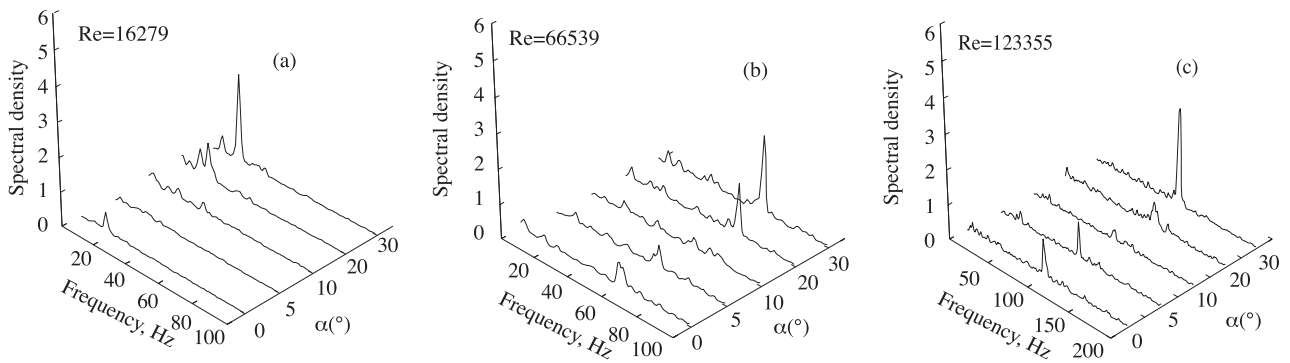


Figure 7. Spectral densities of velocities versus angle of incidence at $x/h=4.0, y/h=0.5$ for square cylinder.

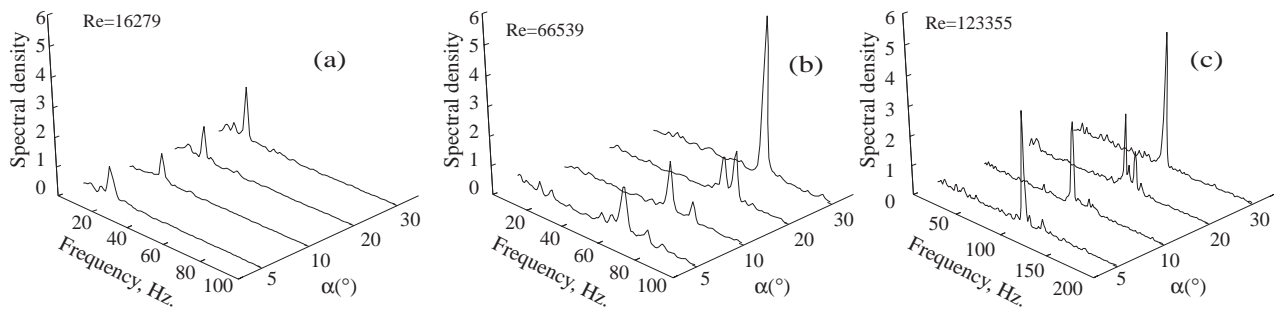


Figure 8. Spectral densities of velocities versus angle of incidence at $x/h=4.0, y/h=-0.5$ for square cylinder.

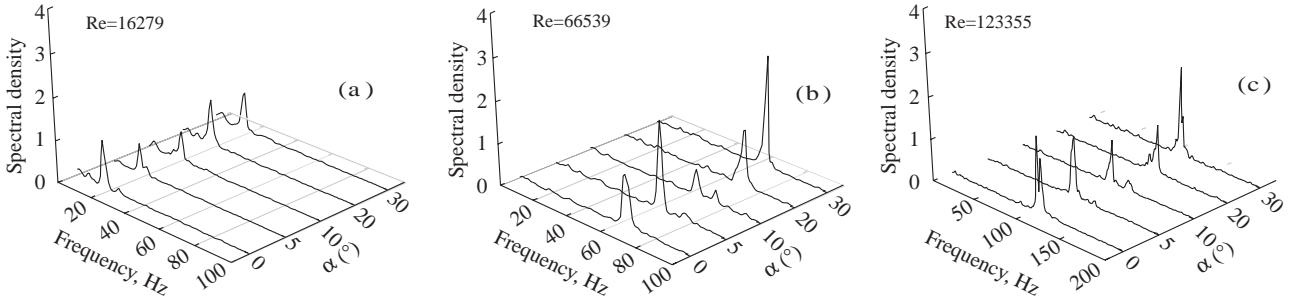


Figure 9. Spectral densities of velocities versus angle of incidence at $x/h=4.0$, $y/h=1.5$ for square cylinder.

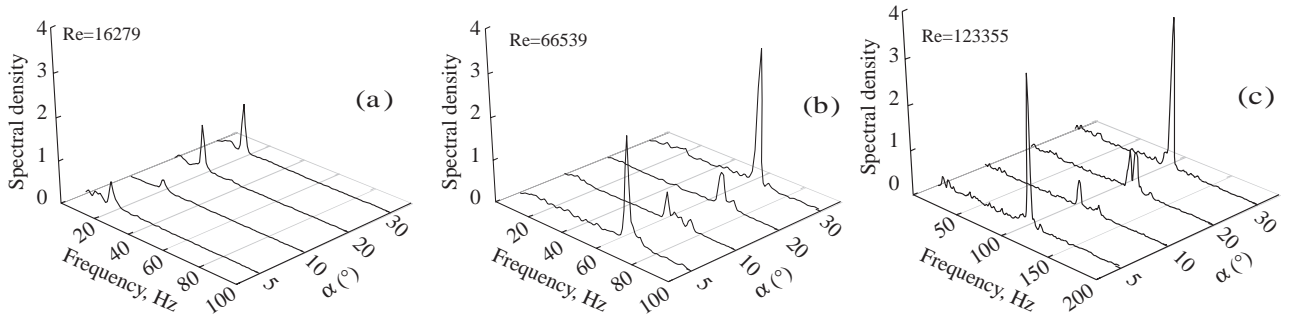


Figure 10. Spectral densities of velocities versus angle of incidence at $x/h=4.0$, $y/h=-1.5$ for square cylinder.

The strouhal numbers obtained in the wake of the square cylinder at the position $x/h = 4$, $y/h = 0.5$ for 0° incidence are plotted in Figure 11 together with data obtained by other investigators. These data exhibit some scatter, which may be attributed to differences in the blockage ratios of various investigators. The blockage ratios reported in the experiments of Mukhopadhyay et al. (1992), the present study, Okajima (1982) and Obasaju (1983) were 12.5%, 10.94%, 7.5%, and 5.5% respectively. As shown in this figure, the Strouhal number increases with increasing blockage ratio as expected.

To see the effects of the w/h ratio of the rectangular cylinder, spectral measurements at various locations in the wake of the rectangular cylinder were performed. Sample results obtained for $w/h = 0.5$ and 2.0 at 0° incidence are presented in Figures 12, 13, 14, 15, 16, and 17. For $w/h = 0.5$, Figures 12 and 13 show that more dominant peaks are detected for a larger value of $y/h (= 0.9375)$ at the same $x/h = 2.5$ station. However, the shedding frequency is nearly constant and is not affected as the y/h increases from 0.3125 to 0.9375.

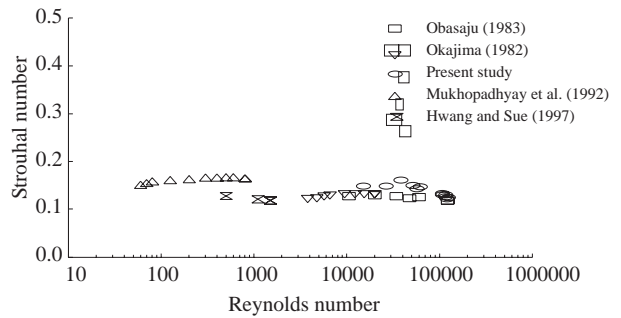


Figure 11. Comparison of Strouhal numbers obtained at $x/h=4$, $y/h=0.5$ at 0° incidence for square cylinder.

Spectral peaks decrease considerably as the value of y/h increases from 0.625 to 1.875 at the stations; $x/h = 2.75$ and 5.0 in the wake of the rectangular cylinder with $w/h = 2.0$ (see Figures 14-17). This is due to the fact that when $w/h = 2.0$, the value of $y/h = 1.875$ is outside the wake of the rectangular cylinder.

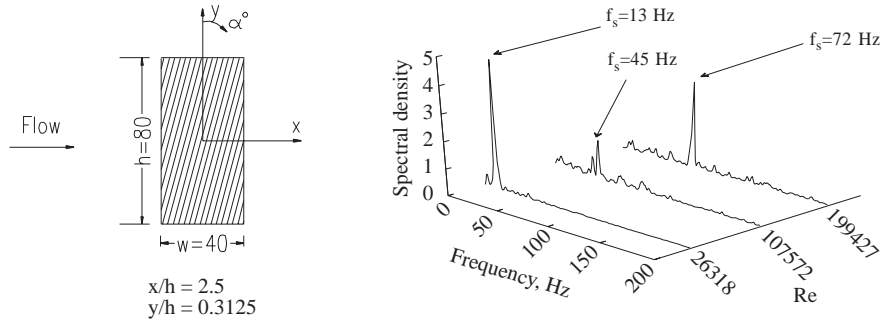


Figure 12. Spectral densities versus Reynolds number at $x/h=2.5$, $y/h=0.3125$ for rectangular cylinder with $w/h=0.5$ and at 0° incidence.

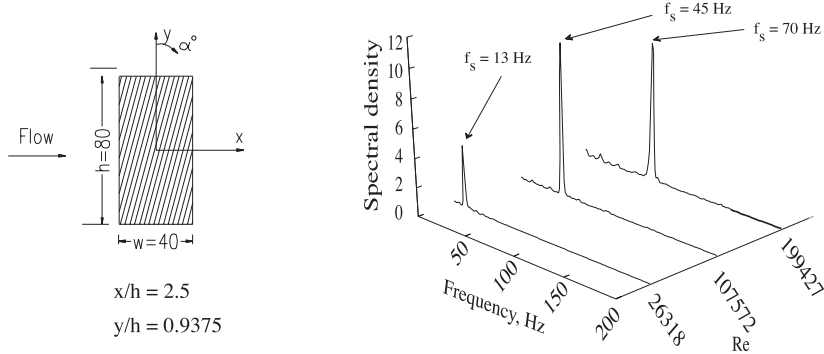


Figure 13. Spectral densities versus Reynolds number at $x/h=2.5$, $y/h=0.9375$ for rectangular cylinder with $w/h=0.5$ and at 0° incidence.

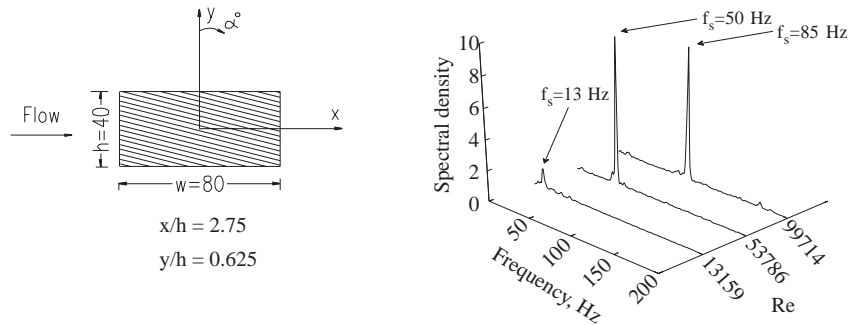


Figure 14. Spectral densities versus Reynolds number at $x/h=2.75$, $y/h=0.625$ for rectangular cylinder with $w/h=2.0$ and at 0° incidence.

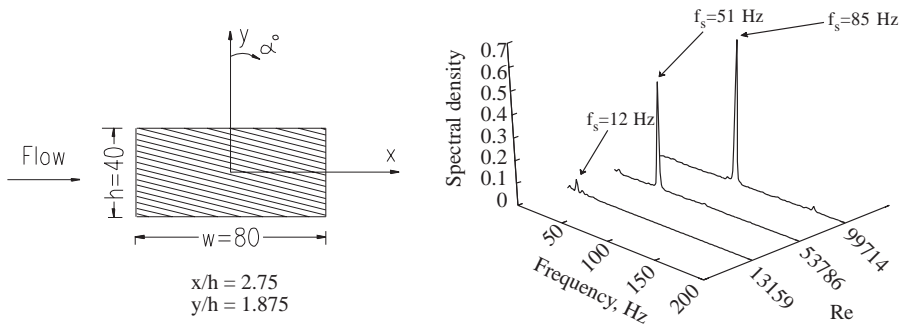


Figure 15. Spectral densities versus Reynolds number at $x/h=2.75$, $y/h=1.875$ for rectangular cylinder with $w/h=2.0$ and at 0° incidence.

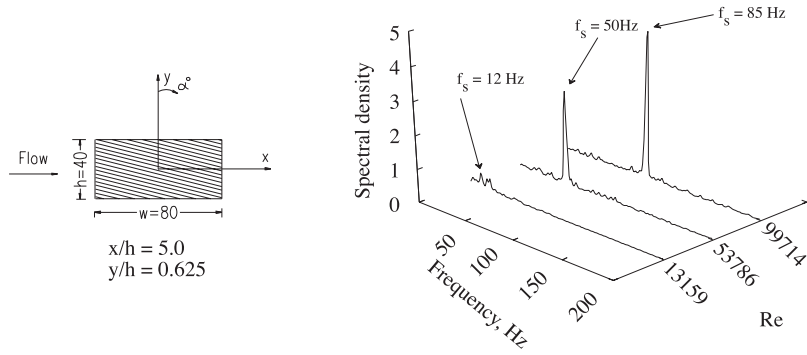


Figure 16. Spectral densities versus Reynolds number at $x/h=5.0$, $y/h=0.625$ for rectangular cylinder with $w/h=2.0$ and at 0° incidence.

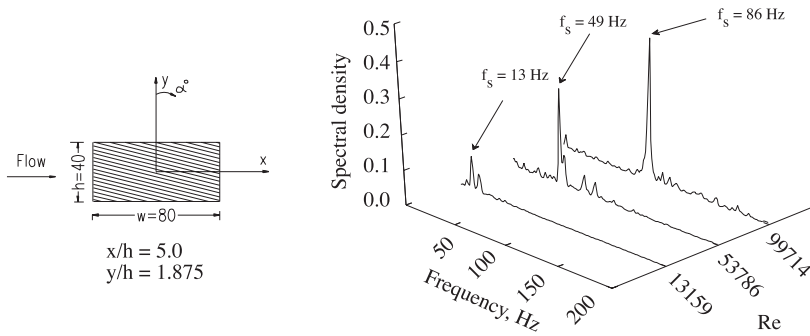


Figure 17. Spectral densities versus Reynolds number at $x/h=5.0$, $y/h=1.875$ for rectangular cylinder with $w/h=2.0$ and at 0° incidence.

Strouhal numbers and shedding frequency parameters determined for rectangular cylinders with $w/h = 0.5$ and $w/h = 2.0$ versus the Reynolds number are logarithmically presented in Figures 18 and

19. As can be seen from these figures, the change in Strouhal number with increasing angle of incidence is more important for the rectangular cylinder with $w/h = 2.0$ than for the cylinder with $w/h = 0.5$.

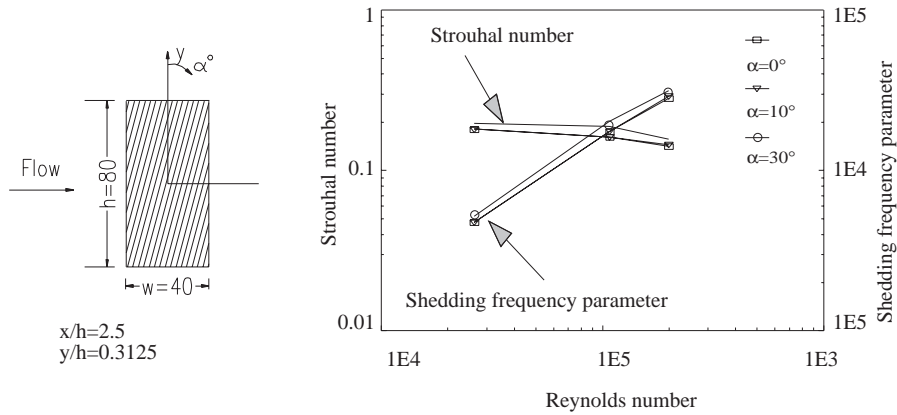


Figure 18. Strouhal number and shedding frequency parameter versus Reynolds number at $x/h=2.5$, $y/h=0.3125$ for rectangular cylinder with $w/h=0.5$.

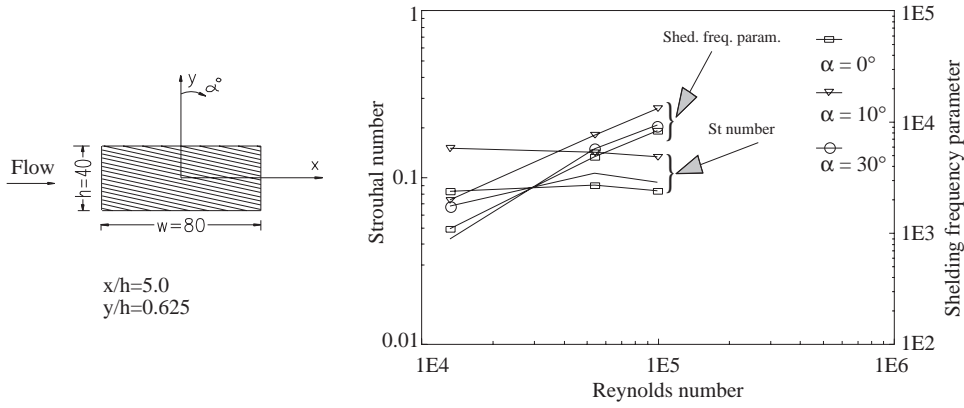


Figure 19. Strouhal number and shedding frequency parameter versus Reynolds number at $x/h=5.0$, $y/h=0.625$ for rectangular cylinder with $w/h=2.0$.

The effects of width-to-height ratio on spectral peaks and Strouhal number are shown in Figure 20.

As shown in this figure, with increasing w/h the spectral peak decreases.

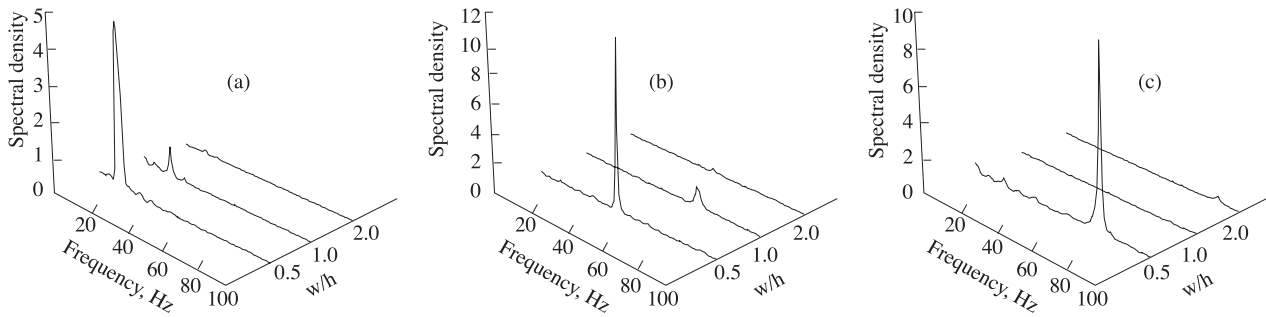


Figure 20. Spectral densities versus w/h for different Reynolds numbers: a) $Re=16279$, b) $Re=66539$ and c) $Re=122355$ (Re number is based on the side of the square cylinder)

This observation is in agreement with the values of Park (1989), who reported that the Strouhal number increases with w/h when $w/h < 0.6$ and decreases for $w/h > 0.6$. The relationship between the Strouhal number St and the width-to-height ratio of rectangular cylinders is given in Figure 21. It may be clearly observed in this figure that the Strouhal number decreases with increasing w/h .

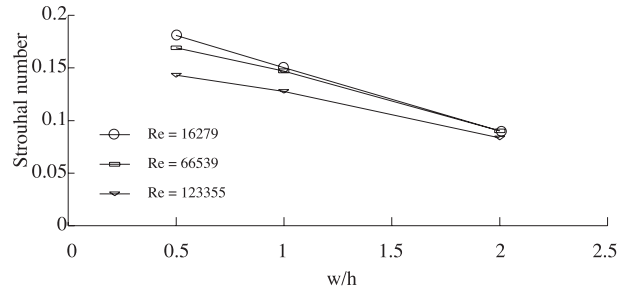


Figure 21. Variation of Strouhal number with w/h for different Reynolds numbers (Re number is based on the side of the square cylinder)

Conclusion

In this paper, vortex shedding from finite length circular and rectangular cylinders, when placed horizontally in cross flow at the mid-height of the test section of a wind tunnel were determined experimentally.

Vortex shedding frequencies increased with increasing Reynolds numbers for all the models tested regardless of their cross section, circular or rectangular, and the corresponding shedding frequency parameters, $F = f_s D^2 / \nu$, increased linearly with the Reynolds number when plotted on a logarithmic

scale.

Strouhal numbers determined for the circular cylinder are about 0.2 in the Reynolds number range $1 \times 10^4 - 2 \times 10^5$ whereas the Strouhal numbers obtained for the square cylinder ($w/h = 1.0$) having the same hydraulic diameter as that of the circular cylinder at 0° incidence were between 0.12 and 0.16. The Strouhal numbers determined for the rectangular cylinders decreased with increasing width-to-height ratios.

It was also observed that the Strouhal numbers increase with increasing blockage ratios whereas the angle of incidence has very little or no effect on the Strouhal numbers.

The spectral density distributions determined in the wake of the models were as follows;

While vortex-shedding frequency is inversely proportional to wake width, shedding intensity is dependent on the stationary character of the vortex sheet. For the circular cylinder, dominant spectral peaks were detected at the location, $y/D = 0.5, x/D = 2.2$ and no peaks were detected in the region above $y/D > 1.5$. For rectangular cylinders, dominant peaks were detected at the locations $y/h = 1.0, x/h = 4.0$ for the cylinder with $w/h = 1.0$ and $y/h = 0.9375, x/h = 2.5$ and $y/h = 0.625, x/h = 2.75$ for cylinders with $w/h = 0.5$ and $w/h = 2.0$ respectively.

Nomenclature

D	: cylinder diameter, m
f	: frequency, Hz
$G_x(f)$: power spectral density function
H	: height of the tunnel section, m
F	: shedding frequency parameter (non-dimensional frequency), $F = f_s D^2 / \nu$ (or $f_s h^2 / \nu$)
L	: length of the model, m
Re	: Reynolds number based on cylinder diameter, $Re = \bar{U} D / \nu$ (or $\bar{U} h / \nu$), dimensionless
St	: Strouhal number, $St = f_s D / \bar{U}$ (or $f_s h / \bar{U}$), dimensionless
\bar{U}	: mean velocity in x-direction, m/s
W	: width of the tunnel section, m
f_s	: vortex-shedding frequency, Hz
h	: height of the model, m
w	: width of the model, m
x, y, z	: streamwise, lateral and spanwise coordinate, m

Greek Symbols

α	: The angle of incidence, $^\circ$
ν	: Kinematic viscosity, m^2/s

References

- Achenbach, E. and Heinecke, E., "On Vortex Shedding From Smooth and Rough Cylinders in the Reynolds Numbers From 6×10^3 to 5×10^6 ", J. Fluid Mech. 109, 239-251, 1981.
- Bearman, R.W., "On Vortex Shedding From a Circular Cylinder in the Critical Reynolds Number Regime", J. Fluid Mech. 37, 577-585, 1969.
- Bearman, P.W. and Trueman, D.M., "An Investigation of the Flow Around Rectangular Cylinders", Aeronautical Quarterly 23, 229-237, 1972.
- Farell, C. and Blessmann, J., "On Critical Flow Around Smooth Circular Cylinders", J. Fluid Mech. 136, 375-391, 1983.
- Gaster, M., "Vortex Shedding From Circular Cylinders at Low Reynolds Numbers", J. Fluid Mech. 46(4), 749-756, 1971.
- Gerich D., Eckelmann, H., "Influence of End Plates and Free Ends on the Shedding Frequency of Circular Cylinders", J. Fluid Mech. 122, 109-121, 1982.
- Hwang, Robert R. and Sue, Y. C., "Numerical Simulation of Shear Effect on Vortex Shedding Behind A Square Cylinder", International Journal For Numerical Methods In Fluids 25, 1409-1420, 1997.
- Kim, H. J., "An Experimental Investigation on the Flow Around a Circular Cylinder in the First Critical Subregion", Ph.D. Thesis, The Faculty of The Graduate School of The University of Minnesota, Minnesota, 1986.
- Mukhopadhyay, A., Biswas, G. and Sundararajan, T., "Numerical Investigation of Confined Wakes Behind a Square Cylinder in a Channel", International Journal For Numerical Methods in Fluids 14, 1473-1484, 1992.
- Nakaguchi, H., Hashimoto, K. and Muto, S., "An Experimental Study on Aerodynamic Drag of Rectangular Cylinders", Journal of the Japan Society of Aeronautical and Space Sciences 16, 1-5, 1968.
- Nishioka, M. and Sato, H., "Measurements of Velocity Distributions in the Wake of a Circular Cylinder at Low Reynolds Numbers", J. Fluid Mech. 65(1), 97-112, 1974.

Obasaju, E.D., "An Investigation of the Effects of Incidence on the Flow Around a Square Section Cylinder", *Aeronautical Quarterly* 34, 243-259, 1983

Okajima, A., "Strouhal Numbers of Rectangular Cylinders", *J. Fluid Mech.* 123, 379-398, 1982.

Park, W.C., "Computation of Flow Past Single and Multiple Bluff Bodies by a Vortex Tracing Method", Ph.D. Thesis, The Faculty of The Graduate School of The University of Minnesota, Minnesota, 1989.

Sakamoto, H. and Arie, M., "Vortex Shedding From a Rectangular Prism and a Circular Cylinder Placed

Vertically in a Turbulent Boundary Layer", *J. Fluid Mech.* 126, 147-165, 1983.

Sax, M.J., "Fluctuating Pressure Field on a Yawed Rigid Cylinder", Ph.D. Thesis, The Faculty of The Graduate School of The University of Minnesota, Minnesota, 1978.

West, G.S., and Apelt, C.J., "The Effects of Tunnel Blockage and Aspect Ratio on the Mean Flow Past a Circular Cylinder With Reynolds Number Between 10^4 and 10^5 ", *J. Fluid Mech.* 114, 361-377, 1982.